SECOND EUROPEAN CONFERENCE ON OPTICAL FIBRE COMMUNICATION.

Communication IV.2

Etude de la propagation pour des fibres monomode en phospho-silicate.

Propagation studies on single-mode phosphosilicate fibres.

W.A. GAMBLING, D.N. PAYNE, H. MATSUMURA
University of Southampton
Southampton SO9 5NH
GRANDE-BRETAGNE

RESUME

On décrit une méthode pour déterminer le diamètre du coeur d'une fibre monomode et la différence d'indice de refraction entre le cœur et l'enveloppe. Cette méthode comporte seulement la mesure de la largeur du lobe principal à demi-puissance et de la largeur du 1^er minimum. Quand une fibre monomode est courbée on trouve que, comme privu, les pertes dues à la courbure croissent brusquement au dela d'un rayon de courbure critique mais que la radiation émergente ne se propage pas uniformément avec la distance; On observe au fait une serie de rais bien définies et distribuées de manière discrète.

ABSTRACT

A method is described for determining unambiguously from the far-field pattern of single-mode fibres the core diameter and the refractive index difference between core and cladding. It involves measurements only of the half-power width of the main lobe and the width of the first minimum. When a single-mode fibre is curved we find that, as expected, the bend loss increases sharply below a critical bend radius but that the radiation does not leak away uniformly with distance. Instead a series of discrete, well-defined rays is observed.

1. Introduction

Single-mode fibres have several potential advantages when considered for use as transmission lines at optical frequencies. In particular the absence of dispersion due to multimode operation means that the attainable bandwidth can be very large, being ultimately limited by material and mode dispersion when operating with a monochromatic source and estimates (1) give values in the region of 100GHz over a 1km length. In recent years attention has centred on multimode fibres because they can be used with light-emitting diodes and they present fewer handling problems, in launching and jointing for example. However the fabrication of single-mode fibres has been rendered comparatively simple (2) by the new homogeneous chemical vapour deposition technique. Furthermore it may be deduced from recent theoretical work (3) that the 'microbending' loss can be made small by restricting the core diameter. Together with the longer lifetimes now being reported for semiconductor lasers, these factors indicate that single-mode fibres may become increasingly important in the future.

2. Determination of core diameter and refractive-index difference

With any type of fibre, two of the fundamental parameters are the core diameter 2a and the difference in refractive index Δn between that of the core n_1 and the cladding n_2 from which the normalised frequency V at the (free-space) wavelength of operation λ may be obtained where

$$V = (2\pi a/\lambda)(n_1^2 - n_2^2)^{\frac{1}{2}}$$

In multimode fibres the core diameter can be measured by conventional optical techniques while Δn can be determined from measurements of the numerical aperture or of the refractive-index profile. However with single-mode fibres, because the core diameter is comparable with a wavelength, the effects of diffraction render such measurements more difficult, particularly at the smaller V values. Sometimes the refractive indices of core and cladding may be accurately known but in general this is not the case, particularly with fibres produced by the C.V.D. technique. A method of determining a and Δn is therefore required which is simple to apply and which ideally can be used to assess fibres immediately after drawing.

No rapid and satisfactory method presently exists. One possible technique is to detect the onset of higher mode propagation in the output far-field radiation pattern from the fibre when the exciting wavelength is varied.

53

In this way the wavelength of the second mode cut-off ($V=2.4$) is found, and assuming that the dispersive properties of the glasses in the core and cladding are similar, an extrapolation of the V value to other wavelengths can be made. However, the method is an insensitive one because the wavelength at which a higher mode appears in the output pattern is somewhat indeterminate. A mode becomes extremely lossy as it nears its cut-off point, since the mode volume becomes large and guidance is weak. Thus no clear cut-off wavelength is observed and the measurement is sensitive to slight bends and applied pressure, as these cause premature radiation of the higher mode. Thus the mode cut-off technique is not sufficiently accurate and, moreover, requires a laser source which is tunable over a wide range of wavelengths.

An alternative method is presented here of determining a and Δn from a simple measurement of the far-field pattern at a single wavelength.

2.1 Far-field radiation pattern of HE_{11} mode

As with multimode fibres it is clear that the far-field radiation pattern of the HE_{11} mode is a function of both a and Δn and moreover can be easily observed experimentally(4). We have calculated this field distribution, assuming $\Delta n \ll n_1$. The normalized far-field distribution $\psi(r,\theta,\phi)$ may be obtained from the Fraunhofer diffraction equation (5) and the approximate field equations derived by Snyder (6). For the HE_{11} mode in structures having $\Delta n \ll n_1$ the normalized far-field distribution may be derived as:

$$|\psi^2| = \left[\frac{U^2\,W^2}{(U^2-\alpha^2)(W^2+\alpha^2)}\left\{J_o(\alpha) - \alpha J_1(\alpha)\frac{J_o(U)}{UJ_1(U)}\right\}\right]^2 \quad \text{for } U \neq \alpha \quad ..(1a)$$

$$= \left[\frac{U^2W^2}{2V^2}\,\frac{1}{UJ_1(U)}\left\{J_o^{\,2}(\alpha) + J_1^{\,2}(\alpha)\right\}\right]^2 \quad \text{for } U = \alpha \quad ..(1b)$$

where $V^2 = U^2 + W^2$.

U,W are the arguments (6) of the Bessel and modified Hankel functions.

$\alpha = ka \sin\theta$ is the normalised radiation angle

$k = 2\pi/\lambda$ and

θ the angle with the axis.

A convenient parameter to measure experimentally is the output angle θ_h at which the far-field intensity has fallen to one-half that at the central maximum ($\theta = 0$).

It may be shown from eqn.(1) that $\alpha_h = ka \sin\theta_h$ is an unambiguous function of V and the relationship is indicated by curve B in Fig.1. Thus V may be very simply determined if α_h is known, assuming that for $V>2.4$ only the HE_{11} mode is launched and propagated along the fibre. If the core radius a can be found in some other way then measurement of the half-intensity width θ_h enables α_h to be obtained, so that eqn.(1), or in practice Fig.1, gives V and hence Δn. An etching technique can sometimes be used to determine the core diameter but only with those fibres where the core and the cladding have markedly different etch rates.

2.2 Angular width of first maximum

The output end of an optical fibre forms a radiating aperture but it is not generally appreciated that the output field pattern contains side lobes. Thus it can be shown from eqn.(1), and experimentally, that in addition to the main beam the far-field pattern exhibits a range of subsidiary peaks, at angles and relative intensities which depend on a, n_1 and λ. It may be further shown that the angular width θ_x to the first minimum can be used in conjunction with θ_h to obtain V directly without any knowledge of a. Thus, like α_h, the ratio $\sin\theta_x/\sin\theta_h$ is also an unambiguous function of V. The variation of this ratio, together with α_h, is given in Fig.1 for the range of V values most likely to be encountered in practical single-mode fibres. Thus the interesting and invaluable result is obtained that the simple determination of θ_x and θ_h enables V and a, and hence Δn to be obtained without the need for any other measurements. In the example illustrated in Fig.1 it is assumed that the ratio ($\sin\theta_x/\sin\theta_h$) is found experimentally to be 5.25 indicating, using curve A, that $V = 2.14$. From curve B it can be seen that the corresponding value of ka $\sin\theta_h$ is 0.813 and from the measured value of θ_h it is possible to calculate a.

2.3 Experimental techniques and verification

Experiments have been carried out on a number of single-mode fibres made by the technique (2) of homogeneous chemical vapour deposition. Laser radiation was launched into a 1m length of each fibre. In order to avoid the propagation of higher-order modes the fibre was slightly curved and cladding strippers were also used.

The angular widths θ_h and θ_x were obtained by monitoring the far-field output pattern with an Integrated Photomatrix Ltd model 7000 scanning photodiode array. Fig.2 shows the outputs from the array displayed on an oscilloscope under conditions of (a) low gain from which θ_h can be measured and (b) high gain, showing the positions of the minima (θ_x). In Fig.2(a) the response of the photodiode array is linear and the Gaussian shape of the main beam can be seen. However in order to show up the first minima in Fig.2(b) the gain is so high as to cause saturation and distortion at smaller angles. The values of θ_x were confirmed by taking photographs of the far-field pattern as shown in Fig.2(c).

As a check on the theory given in Section 2.2 the core diameter can be measured directly in two ways. Firstly by etching with hydrofluoric acid since the phosphosilicate core dissolves much more rapidly than the pure silica cladding. The core diameter was then measured by an optical, or scanning electron microscope. Secondly the core and outside diameters of the preform were measured as well as the overall diameter of the resulting fibre. The fibre core diameter is then given by the product of the preform core diameter and the preform/fibre outside diameter ratio. The agreement between the two methods was very good (within 2%).

Several single-mode fibres having core diameters ranging from 4 to 8.4μm have been tested. In the first set of measurements a Chromatix CMX4 tunable laser was used to vary the V values over the range 1.7 to 3.5. The angle θ_h was determined at wavelengths between 0.42 and 0.9μm for two fibres whose core diameters of 6.6μm and 8.1μm were obtained by etching. The experimental results are shown in Fig.1 and are in excellent agreement with the theory. The V values for these two fibres were found to be 1.98 and 2.78 at $\lambda = 0.63$μm.

In the second set of measurements θ_h and θ_x were measured for a number of fibres. For each fibre the angular measurements were made in ten independent experiments and the repeatability was within $\pm 2\%$. The core diameters of two of the samples were again obtained by etching and the comparison with the far-field measurements is shown in Table 1. The cores were slightly elliptical and the figures in the final column denote the lengths of the major and minor axes. The agreement between the two methods is excellent particularly since the orientation of the fibre ends for the far-field measurements was not known. For the other three samples independent diameter measurements were not made and the results obtained for a and Δn are given in Table 2.

3. Radiation Loss at Bends

One of the important characteristics of propagation in single-mode fibres is the transmission loss which occurs at bends. We have studied this effect in detail and have compared experimental results with those derived from a theoretical model based on a conformal transformation technique. The agreement between theory and experiment is good and the results will be reported elsewhere. As expected the bending loss increases rapidly as the radius of curvature is reduced below a critical value. The radius at which this occurs is typically 4cm for large-core fibres (8μm diameter, V=2), while our more strongly-guiding fibres (4μm diameter, V=2.4) may be bent to a radius of a few millimetres.

In the course of the bend loss studies it was observed that the radiation emitted in the transverse direction at a bend was not continuous but appeared in the form of discrete divergent 'rays'. To illustrate the effect it is convenient to describe the experimental results first before giving a tentative theoretical explanation of this somewhat unexpected result.

3.1 Experimental study of bend radiation

To observe the 'ray' radiation several metres of single-mode, or near-single-mode, fibre were coiled around a drum of given diameter and the HE_{11} mode was excited at the input end by a helium/neon laser operating at 0.633μm in the TEM_{00} mode. The 'near-single-mode' fibre had a normalized frequency V = 2.78 and a core diameter of 9.8μm but only the HE_{11} mode was present after a few metres because of the launching conditions and any higher-order modes present were only weakly bound so that they attenuated rapidly. Normally the radiation emitted from the core at a bend is internally reflected at the outer surface of the cladding and is therefore not easily observed. The 110μm diameter fibre was therefore laid on a glass plate and immersed in liquid paraffin having a refractive index (1.466) slightly higher than that of the cladding. Typical examples of the radiation observed are shown in Fig.3 at bend radii of 12 and 16.5mm. The radiated beams have a finite width varying as a function of the radius of curvature. The number of beams per unit length of curved fibre increases as the bend radius decreases. The number of rays per complete turn of fibre was measured as the normalized ratio core diameter/bend radius was changed from 1.8 to 3×10^{-4} (54 to 33mm bend radius) and was found to be roughly constant as predicted by the theory outlined below. However there are difficulties in measuring accurately the number of rays per unit length.

Although the experiments reported here were conducted on fibres which propagated more than one mode, the discrete radiation emitted from the bend was also observed in truly monomode fibres having V less than 2.4. In addition, smaller-core fibres exhibit the effect at a reduced bend radius. It may be inferred from the work of Neumann (7) that a related phenomenon exists in dielectric waveguides operating at microwave frequencies.

3.2 Analysis of leakage from a curved single-mode fibre

The analysis is based on a conformal transformation (8) which can be used to map a curved homogeneous cylindrical medium into an inhomogeneous linear one in the transform plane. However we assume here for simplicity a curved slab waveguide of half width d, refractive index n_1 and mean radius of curvature R in the plane of curvature (r,θ) as shown in Fig.4(a). This structure is mapped into the (u,v) plane by the transformation

$$u = R\ln(r/R) \qquad v = R\theta \qquad ..(2)$$

in the form of a straight waveguide with the dimensions and refractive-index distribution indicated in Fig.4(b). It is clear that the energy distribution in the curved waveguide is shifted towards the outer curved boundary by the increase of refractive index at the right-hand boundary in the transform plane. The effective fibre diameter in the (u,v) plane becomes

$$D = R\ln\left[(R+d)/(R-d)\right] \qquad ..(3)$$

Both D and the slope of the refractive index in the u direction, $\exp(u/R)$, increase as the curvature increases.

The effect of these changes on the propagation conditions may be deduced from Fig.5. The dotted curve (a) shows the transverse distribution of refractive index in the (u,v) plane for a straight fibre in the (r,θ) plane, i.e. $R = \infty$ so that the width of the guide is the same in both planes, D = 2d, and the refractive index is constant. Also shown is the normalized propagation constant of the HE_{11} mode. Strictly speaking the propagation constant is that of the slab TE_{01} or TM_{01} mode but calculation shows that the propagation constants of the lowest-order modes in slab and fibre are very similar and the approximation is certainly good enough for our purpose here.

At a moderate radius of curvature, solid curve (b), the refractive index at u = d increases from n_1 to $n_1(1+d/R)$ in the core and from n_2 to $n_2(1+d/R)$ in the cladding (see Fig.4). Similarly at the inner radius the refractive index changes from n_1 to $n_1(1-d/R)$ in the core and from n_2 to $n_2(1-d/R)$ in the cladding. As indicated above there is therefore a narrowing accompanied by a shift in the energy density to the outside of the curve. Furthermore for u>d the refractive index increases at the rate $n_2\exp(u/R)$ and exceeds the value β/k at a finite distance from the waveguide. Thus the possibility arises of electromagnetic tunnelling as discussed by Snyder (9) which will give rise to bending loss.

When the bend radius is decreased sufficiently, curve (c), two further effects occur. Firstly, the point can be reached at which $n_2(1+d/R)$ equals or exceeds β/k so that all guidance ceases and the radiation loss rises to infinity. This, and the tunnelling from a curved fibre, are discussed elsewhere (10) and will not be treated further here. However the other effect of importance at a small radius of curvature arises when the effective refractive index in the core, $n_1(1-d/R)$, at the inside of the bend falls below β/k. A turning point (caustic) then forms within the core and since the inner core boundary no longer has a guiding function is ceases to have any relevance. The form of the guiding structure therefore changes from that of a single-mode fibre to a single-boundary guide (11). The HE_{11} mode in the curved fibre may therefore be thought of in terms of the equivalent locus or ray (see for example reference (12)) from the straight portion entering an open curved 'whispering gallery' reflecting region of radius R and with an outer caustic at a distance from the core at which the equality

$$\beta/k_2 = n_2 \exp(u/R)$$

is satisfied and through which tunnelling radiation is emitted as in Fig.6. The characteristic angle of the ray can be shown to be

$$\theta_c = \text{arc cos}\left[U\lambda/2\pi n_1 d\right]$$

where U is the eigenvalue of the HE_{11} mode in the straight single-mode fibre. Thus the theory predicts the emission of tangential rays at the points of reflection of the HE_{11} 'ray' as illustrated in Fig.6. The number of rays per unit length is a function of θ_c and R, and it can be shown quite simply from the geometric reflection model that the number of emitted rays per complete turn is almost independent of the normalized inverse bend radius d/R.

As described in Section 3.2 such rays are indeed observed and the number per turn is in approximate agreement with the theoretical predictions.

4. Conclusions

It has been shown that the core diameter and refractive index difference can be deduced from the far-field radiation pattern of the HE_{11} mode in fibres of low V number. Independent determinations of the core diameter by an etching technique, as well as by measurements on the starting preform which is made by the homogeneous CVD process, are in good agreement with those obtained from the far-field pattern. The method is now used in our laboratories for the routine characterization of single-mode fibres.

A study of the radiation loss from a curved fibre carrying only the dominant mode indicates that it is composed of discrete beams which may be described as geometrical reflections of the leaky HE_{11} mode at the curved fibre boundary. An analysis based on a conformal transformation technique is presented and gives a satisfactory explanation of the experimental observations. The experimental and theoretical results are also in fairly good quantitative agreement.

Acknowledgements

We are indebted to Dr.C.R.Hammond and Mr. S.R.Norman for fabricating the fibres used in the experiments and to the Pirelli General Cable Company for the endowment of research fellowships. Grateful acknowledgement is also made to Mr. R.B.Dyott for discussions leading to the results outlined in Section 2.2.

References

1. Kapron,F.P. and Keck,D.B.:'Pulse transmission through a dielectric optical waveguide', Appl.Optics, 1971, 10, pp 1519-1523.
2. Gambling,W.A., Payne,D.N., Hammond,C.R. and Norman,S.R.:'Optical fibres based on phosphosilicate glass', Proc.IEE, 1976, 123 (6) pp 570-576.
3. Petermann,K.:'Microbending loss in monomode fibres', Electron.Lett. 1976, 12, pp 107-109.
4. Kapany,N.S.:'Fiber Optics',(Academic Press, 1967)Chap.14, p 327.
5. Born,M. and Wolf,E.:'Principles of Optics' (Pergamon Press, 1970), p 370.
6. Snyder, A.W.:'Asymptotic expressions for eigenfunctions and eigenvalues of a dielectric or optical waveguide', IEEE Trans.,1969, MTT-17, pp 1130-1137.
7. Neumann,E.G. and Rudolph,H.D.:'Losses from corners in dielectric-rod or optical-fiber waveguides', Appl.Phys.,1975, 8,pp 107-116.
8. Maurer,S.J. and Felsen,L.B.:'Ray methods for trapped and slightly leaky modes in multi-layered or multi-wave regions', IEEE Trans.,1970, MTT-18, pp 584-595.
9. Snyder,A.W. and Love,J.D.:'Reflection at a curved dielectric interface - Electromagnetic tunnelling', IEEE Trans., 1975, MTT-23, pp 134-141.
10. Gambling,W.A., Payne,D.N. and Matsumura,H.: (to be published)
11. Wait,J.R.:'Electromagnetic whispering gallery modes in a dielectric rod', Radio Science, 1967, 2, pp 1005-1017.
12. Gambling,W.A., Payne,D.N. and Matsumura,H.: 'Theoretical analysis of curved waveguide', AGARD Symposium on Electromagnetic Wave Propagation Involving Irregular Surfaces and Inhomogeneous Media, The Hague, 1974.

TABLE 1 Comparison of core diameters obtained from far-field pattern with those measured by etching

Sample	$\sin\theta_h$ (mean)	$\sin\theta_x/\sin\theta_h$ (mean)	V (mean)	Δn	Core diameter (μm) obtained from: Far-field measurements	Etching measurements
1	0.0211	5.38	2.10	0.00107	7.6	7.36 x 7.82
2	0.0385	5.14	2.18	0.00349	4.3	4.22 x 4.31

TABLE 2 Values of V, refractive index difference and core diameter determined from the far-field pattern

Sample	$\sin\theta_h$ (mean)	$\sin\theta_x/\sin\theta_h$ (mean)	V (mean)	Δn	Core diameter μm
3	0.0205	6.05	1.91	0.00108	6.9
4	0.0220	4.79	2.32	0.00112	8.2
5	0.0231	4.50	2.48	0.00120	8.4

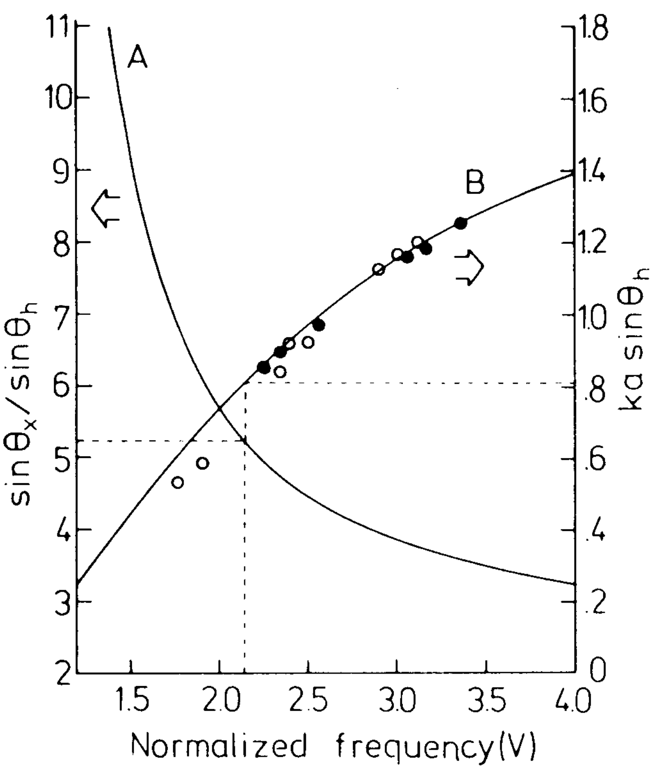

FIG.1. VARIATION OF THE NORMALISED HALF-INTENSITY ANGLE α_h AND THE RATIO ($\sin\theta_x/\sin\theta_h$) WITH V. THE SOLID LINES ARE CALCULATED USING EQN.1 WHILE THE POINTS WERE MEASURED WITH FIBRES OF CORE DIAMETER 6.[illegible]μm (o) AND 8.1μm (●) OVER THE WAVELENGTH RANGE 0.4[illegible]μm TO [illegible]μm

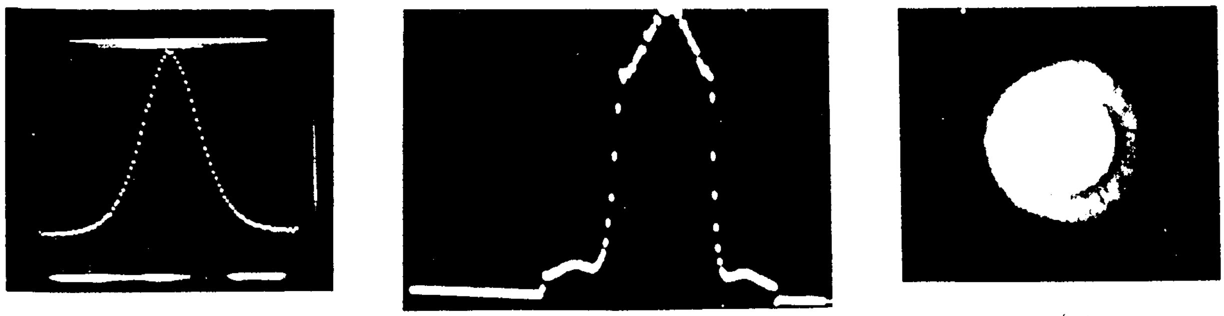

(a) (b) (c)

FIG.2 OUTPUT FROM SCANNING PHOTODIODE ARRAY

a) UNDER LOW-GAIN CONDITIONS
b) UNDER HIGH-GAIN CONDITIONS. NOTE THAT THE CENTRAL PEAK IS SATURATED
c) PHOTOGRAPH OF THE FAR-FIELD INTENSITY PATTERN

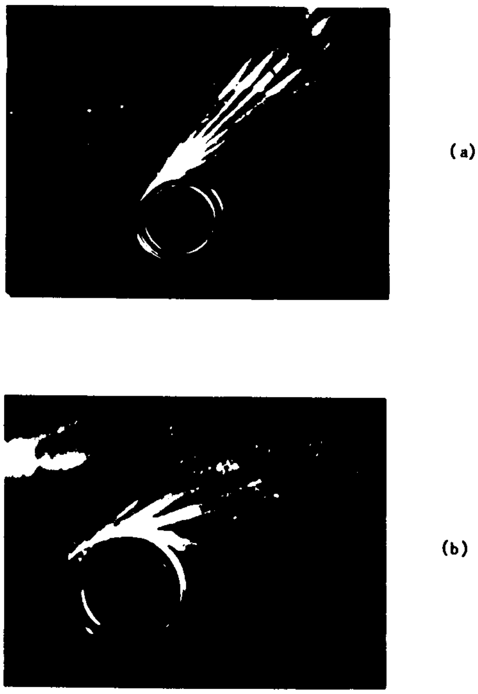

FIG.3 TANGENTIAL BEAMS EMITTED BY A SINGLE-MODE FIBRE AT BEND RADII OF (a) 12MM AND (b) 16.5MM

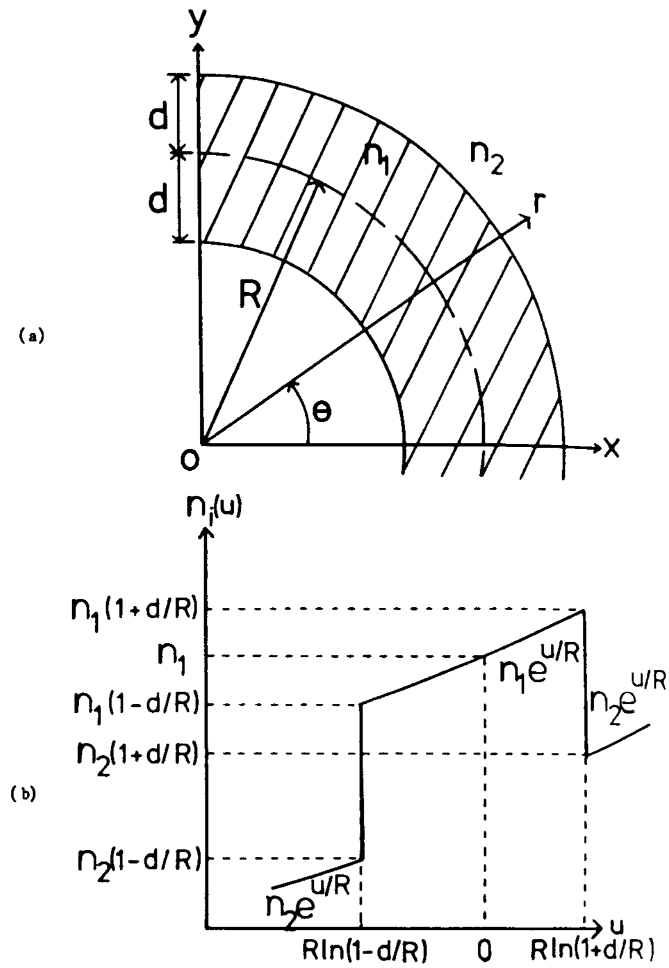

FIG. 4 (a) REPRESENTATION OF A CURVED SLAB WAVEGUIDE IN THE (r,θ) PLANE.
(b) VARIATION OF REFRACTIVE INDEX WITH U IN THE TRANSFORM

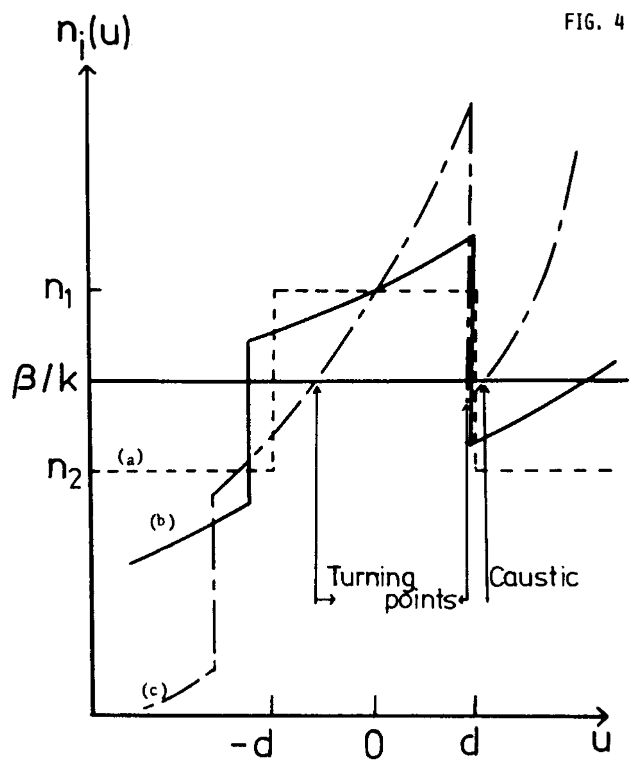

FIG. 5 CHANGE OF REFRACTIVE INDEX IN THE TRANSFORM PLANE FOR (a) ZERO, (b) MODERATE AND (c) LARGE CURVATURES.

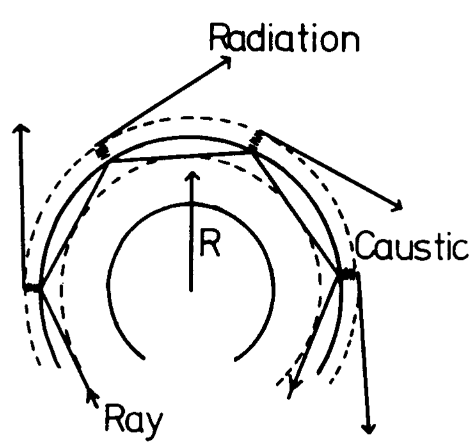

FIG. 6 ILLUSTRATION OF THE TWO CAUSTICS, 'RAY' REFLECTION AND TUNNELLING RADIATION IN A CURVED FIBRE.